A GENETIC DISSECTION OF

MITOCHONDRIAL RESPIRATORY CHAIN BIOGENESIS

An Undergraduate Research Scholars Thesis

by

AARON GRIFFIN, SARAH THERIAULT, SHRISHIV TIMBALIA

Submitted to Honors and Undergraduate Research
Texas A&M University
in partial fulfillment of the requirements for the designation as an

UNDERGRADUATE RESEARCH SCHOLAR

Approved by
Research Advisor: Dr. Vishal Gohil

May 2014

Major: Biochemistry, Genetics
Biochemistry
Biochemistry

TABLE OF CONTENTS

ABSTRACT

A Genetic Dissection of Mitochondrial Respiratory Chain Biogenesis. (May 2014)

Aaron Griffin, Sarah Theriault, Shrishiv Timbalia
Department of Biochemistry and Biophysics
Texas A&M University

Research Advisor: Dr. Vishal Gohil
Department of Biochemistry and Biophysics

Mitochondria house the mitochondrial respiratory chain (MRC), the main site for cellular respiration and energy production. The MRC consists of five large protein complexes (I-V) in the inner mitochondrial membrane. Despite the fundamental role of the MRC in cellular energy generation and its involvement in several human diseases, we still do not know all the proteins required for its formation. To address this gap in our knowledge, we have developed an integrative approach based on clues from evolutionary history and protein localization to shortlist 56 uncharacterized proteins that are physically localized to the mitochondria of yeast and humans. A recent study on mitochondrial disease patients identified potential pathogenic mutations in one of our prioritized candidate genes, *C1orf31*, suggesting its involvement in MRC biogenesis. Due to the lack of an assigned function to C1orf31, it was not possible to prove the pathogenicity of the patient mutations. Therefore, our study focused on determining the role of C1orf31 in MRC biogenesis. We identified a yeast, *Saccharomyces cerevisiae*, ortholog of C1orf31, named Coa6, by BLAST analysis, allowing us to use this genetically tractable model system to quickly decipher the protein's function. Using *coa6Δ* yeast cells, we show that Coa6 is required for respiratory growth, cellular respiration, and MRC complex IV biogenesis. A sequence analysis of Coa6 identified a conserved, non-canonical, putative copper-binding motif,

suggesting its role in copper delivery to MRC complex IV, the only copper-containing MRC complex. Indeed, copper supplementation rescues the respiratory defect of *coa6Δ* yeast cells, while copper starvation exacerbates the respiratory growth phenotype. Furthermore, we show that conserved residues in the putative copper-binding motif, including the residues mutated in the human mitochondrial disease patient, are essential for Coa6 function, thus confirming the pathogenicity of the patient mutations. Based on these results, we hypothesize that Coa6 is a mitochondrial copper metallochaperone required for delivery of copper to MRC complex IV. In support of this hypothesis, we show that the *coa6Δ* phenotype is exacerbated when the gene for another known copper metallochaperone, Sco2, is deleted, indicating that these two proteins have an overlapping function in delivering copper to MRC complex IV.

CHAPTER I

INTRODUCTION

The mitochondrial respiratory chain (MRC) represents an evolutionarily conserved pathway of cellular energy generation. The MRC machinery consists of ~90 core subunits organized into five macromolecular complexes (complexes I-V) that are located in the mitochondrial inner membrane (Fig. 1). Of the 90 MRC subunits, only 13 are encoded by mtDNA. The rest are encoded by the nuclear genome, as are all of the other ~1000 protein components of the mitochondrion (1). The nuclear-encoded proteins are required for the replication and expression of mtDNA-encoded proteins, as well as the full assembly and maturation of the MRC (Fig. 1). Many of the proteins necessary for mtDNA maintenance, transcription, translation, and assembly of a fully operational MRC are currently unknown (1,2). Together, these proteins are commonly referred to as "MRC biogenesis" or "MRC assembly" factors.

Mutations in genes required for building the MRC result in the most common inborn errors of metabolism with an estimated prevalence of 1 in 5,000 live births (3,4). Mitochondrial disease patients display a wide array of symptoms in vital organ systems – including heart defects, strokes, seizures, muscle weakness, deafness, and blindness – underlying the fundamental importance of MRC function to human health (3).

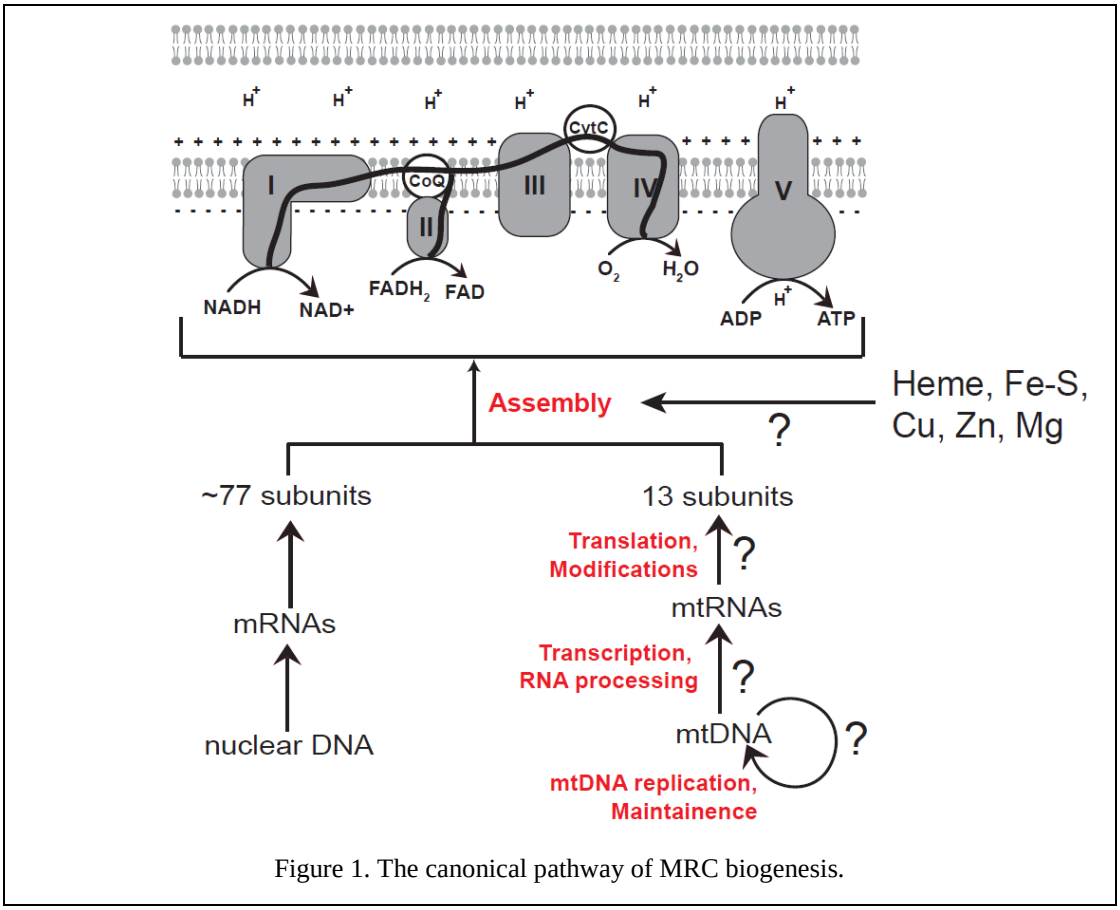

Figure 1. The canonical pathway of MRC biogenesis.

It is necessary to identify the full complement of MRC biogenesis factors in order to completely understand the fundamental process of cellular energy production and to address biomedical challenges stemming from mitochondrial disorders. Most high-throughput studies aimed at identifying MRC biogenesis factors have been performed using *Saccharomyces cerevisiae* yeast deletion strains. For example, combining computational and functional genomic approaches, Caudy et al. identified 100 new yeast mitochondrial proteins whose deficiency alters mitochondrial biogenesis (5). These studies in yeast indicate the presence of a large number of mitochondrial proteins dedicated to MRC biogenesis. Thus, in order to discover novel MRC biogenesis factors, it is useful to know the identity of all the mitochondrial proteins. The most

updated and accurate list of human mitochondrial proteins, termed "MitoCarta," consists of 1,023 proteins (6). Approximately one quarter of the proteins listed in this inventory do not have an assigned function (Fig. 2A). Because of their mitochondrial localization, these 'orphan' proteins provide an excellent starting point for discovering novel MRC biogenesis factors.

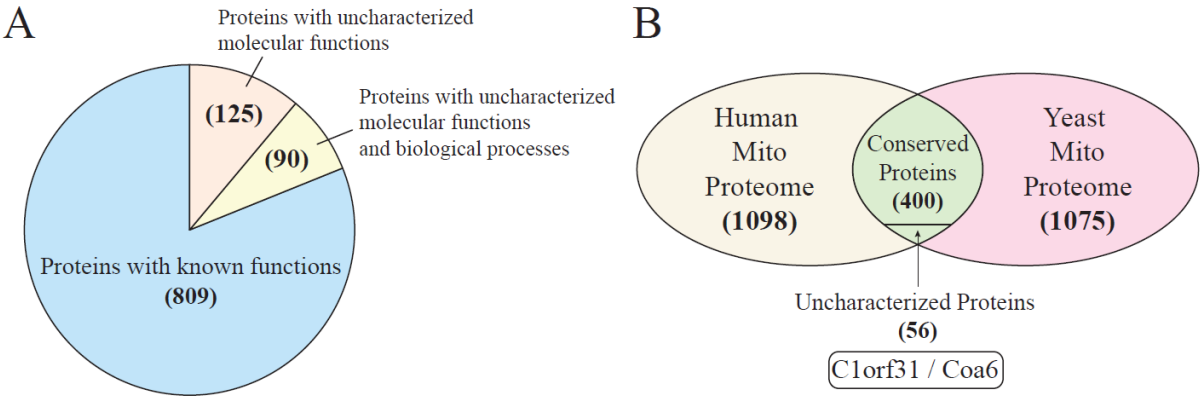

Figure 2. An integrative genomics approach to identify novel MRC biogenesis factors. (A) Pie chart showing the proportion of human mitochondrial proteins with unknown function. (B) Venn diagram showing the 400 evolutionarily conserved mitochondrial proteins between yeast and humans, 56 of which are uncharacterized. C1orf31/Coa6, the prioritized MRC biogenesis candidate, was selected from this subset.

Using these 'orphan' mitochondrial proteins as a starting point, we have designed an integrative genomics approach focused on identifying novel MRC biogenesis factors. Our approach is based on the premise that factors required for building a conserved pathway for mitochondrial ATP synthesis should also be highly conserved and localized to the mitochondria. Using the MitoCarta protein inventory as a starting point, we performed BLAST analyses to shortlist mitochondrial proteins of unknown function that are conserved between yeast and humans. We found that, of the ~400 conserved mitochondrial proteins, 56 are completely uncharacterized (Fig. 2B). This shortlist of 56 evolutionarily conserved 'orphan' mitochondrial proteins should theoretically be highly enriched in novel MRC biogenesis factors. To prioritize shortlisted

proteins for further experimental analysis, we intersected our list with recently reported human mitochondrial disease genes identified through next-generation sequencing. One of the shortlisted genes, *C1orf31*, now renamed *COA6*, was recently linked to a clinical case of neonatal hypertrophic cardiomyopathy in a mitochondrial disease patient (7), suggesting that it likely plays a critical role in MRC function and/or formation. In the study, Calvo and colleagues used next-generation sequencing technologies to identify potential pathogenic mutations in *C1orf31* of the mitochondrial disease patient (7). However, due to the lack of an assigned function to C1orf31, it was not possible to determine if the mutations were responsible for the patient's cardiomyopathy. Due to its evolutionary conservation, its uncharacterized status, and its relevance in a clinical case of mitochondrial disease, we hypothesized that C1orf31/COA6 is a novel MRC biogenesis factor, and set out to investigate its role in MRC function and/or formation.

CHAPTER II

MATERIALS AND METHODS

Yeast strains, plasmids, and culture conditions

Saccharomyces cerevisiae strains used in this study were obtained from Open Biosystems or independently created in the Gohil Laboratory as described below (Table 1). All strains were confirmed by PCR as well as by replica plating on dropout plates. For growth in liquid medium, yeast cells were pre-cultured in YPD (1% yeast extract, 2% peptone and 2% glucose) and then inoculated into medium containing either 2% glucose (YPD) or 3% glycerol + 1% ethanol (YPGE) and grown to early stationary phase. Solid YPD and YPGE media were prepared by the addition of 2% agar. For metal supplementation experiments, growth medium was supplemented with 5 µM divalent chloride salts of Cu, Co, Mg, or Zn. A Gateway cloning vector pAG423-GPD-ccdB-HA (Addgene) was used to perform site-directed mutagenesis (Agilent Technologies QuikChange Lightning) for generating all the point mutants. All constructs were confirmed by DNA sequencing. Yeast cells transformed with the pAG423GPD-ccdB-HA vector were pre-cultured in 2% glucose-containing synthetic media lacking histidine before plating on YPGE.

Table 1
Yeast strains used in this study

Strain	Genotype	Source
*coa6*Δ	Mat α, his301, leu200, lys200, ura300, *coa6*Δ::clonNAT	This study
*cox17*Δ	Mat a, his301, leu200, met1500, ura300, *cox17*Δ::hygro	This study
*cox11*Δ	Mat a, his301, leu200, met1500, ura300, *cox11*Δ::KanMX4	Open Biosystems
*cox12*Δ	Mat a, his301, leu200, met1500, ura300, *cox12*Δ::KanMX4	Open Biosystems
*cox19*Δ	Mat a, his301, leu200, met1500, ura300, *cox19*Δ::KanMX4	Open Biosystems
*cox23*Δ	Mat a, his301, leu200, met1500, ura300, *cox23*Δ::KanMX4	Open Biosystems
*cmc1*Δ	Mat a, his301, leu200, met1500, ura300, *cmc1*Δ::KanMX4	Open Biosystems
*cmc3*Δ	Mat a, his301, leu200, met1500, ura300, *cmc3*Δ::KanMX4	Open Biosystems
*cmc4*Δ	Mat a, his301, leu200, met1500, ura300, *cmc4*Δ::KanMX4	Open Biosystems
*sco1*Δ	Mat a, his301, leu200, met1500, ura300, *sco1*Δ::KanMX4	Open Biosystems
*sco2*Δ	Mat a, his301, leu200, met1500, ura300, *sco2*Δ::KanMX4	Open Biosystems
*pic2*Δ	Mat a, his301, leu200, met1500, ura300, *pic2*Δ::KanMX4	Open Biosystems
STY1 (*cox17*Δ*coa6*Δ)	Mat a, his301, leu200, ura300, lys200, met1500, *cox17*Δ::hygro, *coa6*Δ::clonNAT	This study
STY2 (*cox11*Δ*coa6*Δ)	Mat a, his301, leu200, ura300, *cox11*Δ::KanMX4, *coa6*Δ::clonNAT	This study
STY3 (*cox12*Δ*coa6*Δ)	Mat a, his301, leu200, ura300, lys200, met1500, *cox12*Δ::KanMX4, *coa6*Δ::clonNAT	This study
STY4 (*cox19*Δ*coa6*Δ)	Mat a, his301, leu200, ura300, lys200, *cox19*Δ::KanMX4, *coa6*Δ::clonNAT	This study
STY5 (*cox23*Δ*coa6*Δ)	Mat a, his301,leu200, ura300, *cox23*Δ::KanMX4, *coa6*Δ::clonNAT	This study
STY6 (*cmc1*Δ*coa6*Δ)	Mat a, his301, leu200, ura300, lys200, *cmc1*Δ::KanMX4, *coa6*Δ::clonNAT	This study
STY7 (*cmc3*Δ*coa6*Δ)	Mat α, his301, leu200, ura300, *cmc3*Δ::KanMX4, *coa6*Δ::clonNAT	This study
STY8 (*cmc4*Δ*coa6*Δ)	Mat α, his301, leu200, ura300, lys200, *cmc4*Δ::KanMX4, *coa6*Δ::clonNAT	This study
STY9 (*sco1*Δ*coa6*Δ)	Mat a, his301, leu200, ura300, met1500, *sco1*Δ::KanMX4, *coa6*Δ::clonNAT	This study
STY10 (*sco2*Δ*coa6*Δ)	Mat a, his301, leu200, ura300, lys200, *sco2*Δ::KanMX4, *coa6*Δ::clonNAT	This study
STY11 (*pic2*Δ*coa6*Δ)	Mat a, his301, leu200, ura300, met1500, *pic2*Δ::KanMX4, *coa6*Δ::clonNAT	This study

Primer sequences for knockout cassette PCR amplification were determined using 45 bp upstream and 45 bp downstream of the open reading frame of the gene of interest, as well as 15 bp sequence homologous to the drug resistant cassettes (Table 2). The cassettes used were hphMX4 (resistant to hygromycin) and natMX4 (resistant to clonNAT). Plasmids were extracted from *E. coli* using the Qiagen plasmid prep kit (Cat. #27104) and the DNA concentration was measured using a nanodrop (Thermo Scientific Nanodrop 1000). PCR was performed in order to amplify the cassettes from the plasmids by using the plasmid template, 10x polymerase buffer, the forward primer, the reverse primer, the dNTP mix, the Taq polymerase, and water. DMSO was added when amplifying the natMX4 cassette due to its high GC content. After PCR, agarose gel electrophoresis was performed in order to obtain the DNA of interest. This band of DNA was cut out using the Qiagen gel extraction kit (Cat. #28704) and the DNA concentrations were recorded using a nanodrop (Thermo Scientific Nanodrop 1000). The cassette PCR products were transformed into *S. cerevisiae* using the One Step Transformation protocol and spread onto YPD media plates. The transformation lawns were then replica plated onto media containing hygromycin and clonNAT. The colonies that grew on these plates were then genotyped (Table 1) and checked for accurate gene deletion by PCR (Table 3).

Table 2
Primer sequences for knockout cassette PCR amplification

Primer	Primer Sequence (5' - 3')
COA6 S1	ATACACGAATATACAGAAAGGAATAGTAGTAATATAGCGATGCGTACGCTGCAGGTCGAC
COA6 S2	ATATATATGTTAATATGAGCCAATAACTCACTAAAAACTCAATCGATGAATTCGAGCTCG
COX17 S1	GTGTACACAATCAGATAACTACACAATCAATTATACCCAATGCGTACGCTGCAGGTCGAC
COX17 S2	ATATACAAGAAATGGTTGTCGGCAGACTGTCAGTAAGACTAATCGATGAATTCGAGCTCG

Yeast growth measurements

Growth curves were carried out in glucose containing fermentable media (YPD) and glycerol-ethanol containing non-fermentable media (YPGE). Yeast cells were precultured in 2 ml of YPD media in snap cap tubes for 16 to 20 hours at 30°C and 250 RPM. The next day, the optical density of the preculture was taken using a spectrophotometer (Beckman Coulter DU 730). The preculture was diluted to an initial OD of 0.1 in 7.5 ml YPGE or YPD in 50 ml Falcon tubes; the tubes were then placed in an incubator-shaker at 30°C and 250 RPM. At the specified time points, the optical density of the media was measured by aliquoting 500 µl into cuvettes (VWR 97000-586). If the optical density was beyond the linear range of the instrument (0.05 to 0.800), the samples were diluted.

Spotting was utilized as a method of qualitatively evaluating growth under different conditions. Cell number of overnight precultures of yeast strains were counted by hemocytometer and were serially diluted at 10^4, 10^3, 10^2, and 10^1 cells per 3 µl. Dilutions were spotted onto plates containing different media as indicated and incubated at 30°C or 37°C for 2-5 days.

Streaking was utilized as an additional method of qualitatively evaluating growth under different conditions. Single colonies of yeast strains were isolated and streaked onto media plates, then incubated at 30°C or 37°C for 2-5 days.

Yeast oxygen consumption and mitochondrial isolation

BY4741 WT and *coa6Δ* cells were grown in YPD media to late log phase and then washed, counted, and resuspended in the assay medium (0.176% yeast nitrogen base, 0.5% NH_4SO_4 and 2% ethanol) before seeding in XF24-well microplates (Seahorse Bioscience) at 5 x 10^5 cells/well. After seeding, cells were centrifuged at 100 x g for 2 min and incubated at 30°C for 30 min in the assay medium prior to measurements. The cellular oxygen consumption rate (OCR) was measured using an XF24 extracellular flux analyzer (Seahorse Biosciences) at 30°C. Mitochondria were isolated from yeast cells grown to late log phase in YPD by the previously described method (8) and protein concentrations were determined by the BCA assay (Thermo Scientific). Mitochondrial samples were stored at -80°C before performing any protein analysis.

SDS-PAGE and Western blotting

Denaturing sodium dodecyl sulphate polyacrylamide gel electrophoresis (SDS-PAGE) was performed to separate denatured MRC protein complexes. SDS-PAGE was performed on mitochondrial samples solubilized in RIPA lysis buffer (150 mM NaCl, 1 mM EDTA, 50 mM Tris HCl pH 7.4, 1% NP-40, 0.5% sodium deoxycholate and 0.1% SDS) supplemented with protease inhibitor cocktail (Roche Diagnostic). Western blot was performed using a Trans-Blot transfer cell (Bio-Rad). Membranes were blocked in 5% fatty acid free BSA dissolved in Tris-buffered saline with 0.1% Tween 20 (TBST-BSA) and probed with antibodies as indicated. The separated proteins were blotted onto a polyvinylidene difluoride membrane and blocked for 1h at room temperature in TBST-BSA. Membranes were incubated with primary antibody in TBST-

BSA overnight at 4°C. The primary antibodies for yeast were used at the following dilutions: Cox2, 1:1,000 (Abcam 110271); Cox3, 1:1,000 (Abcam 110259); Sdh2, 1:5,000 (from Dr. Dennis Winge); Rip1, 1:50,000 (from Dr. Vincenzo Zara); Atp2, 1:40,000 (from Dr. Sharon Ackerman); Porin, 1:1,000 (Abcam 110326). Membranes were developed using Western Lightning Plus-ECL (PerkinElmer).

Sporulation, tetrad dissection, and genotyping

Diploid strains were grown in an overnight culture of YPD at 30°C while shaking at 250 rpm. The culture was then diluted by a factor of 1:50 and left to grow for 4 hours while shaking at 30°C. The culture was spun down, washed with sterile water, and resuspended in 2mL of sporulation media, composed of potassium acetate, yeast extract, dextrose, uracil, adenine, leucine, lysine, methionine, histidine, tryptophan, threonine, and arginine. This new culture was then stored at room temperature with shaking for one day and incubated at 30°C with shaking for 4-5 days, or until a sufficient number of tetrads was observed using a tetrad dissection microscope.

Tetrad dissection was performed to obtain haploid spores from tetrads formed during sporulation. The enzyme lyticase (Cat. #SLBD1179V from Sigma) at 0.5 mg/mL in 1 M sorbitol solution was used to digest the cell walls of tetrads, allowing for easier dissection. Following the addition of lyticase, a wide-bore pipette tip was used to deposit 30 µL of culture down the center of a YPD plate. Using a Nikon Eclipse Ci microscope customized with tetrad dissecting arm and stage, tetrads were located, and spores were isolated and redistributed at separate coordinates

along a horizontal line using a fine glass needle. This process was repeated for ~18 different tetrads and the plate was then stored for 2-3 days at 30°C for spores to grow.

After the tetrad dissection, each spore was isolated and transferred to a fresh YPD plate. This master plate was incubated at 30°C and subsequently used to replica plate onto media containing selective markers for genotyping. Synthetic media plates used in this process include CSM (complete synthetic media with Glucose), CSHis (CSM that lacks the amino acid histidine), CSLys (CSM that lacks the amino acid lysine), CSLeu (CSM that lacks the amino acid leucine), CSUra (CSM that lacks the amino acid uracil), and CSMet (CSM that lacks the amino acid methionine). YPD plates with the antibiotic hygromycin, CSM plates with the antibiotic clonNAT, and YPD plates with the antibiotic geneticin were used to determine which haploid spores received which deletion cassette. Finally, CSM lacking all amino acids was used to determine the mating type of each haploid spore. Double knockout strains were confirmed by PCR (Table 3).

Table 3
PCR confirmation of yeast knockout strains

Yeast Strain	Primers	Observed Band Size	Expected Band Size (bp)
WT	Coa6A/Coa6D	~910	898
WT	Cox17A/Cox17D	~1000	1006
STY1 (*coa6*Δ *cox17*Δ)	Cox17A/Cox17D	~2300	2300
	Coa6A/Coa6D	~1800	1800
WT	Cox11A/Cox11D	~1400	1408
STY2 (*coa6*Δ *cox11*Δ)	Cox11A/Cox11D	~2000	2089
	Coa6A/Coa6D	~1800	1800
WT	Cox12A/Cox12D	~750	828
STY3 (*coa6*Δ *cox12*Δ)	Cox12A/Cox12D	~2000	2160
	Coa6A/Coa6D	~1800	1800
WT	Cox19A/Cox19D	~900	900
STY4 (*coa6*Δ *cox19*Δ)	Cox19A/Cox19D	~2100	2215
	Coa6A/Coa6D	~1800	1800
WT	Cox23A/Cox23D	~1000	1036
STY5 (*coa6*Δ *cox23*Δ)	Cox23A/Cox23D	~2000	2164
	Coa6A/Coa6D	~1800	1800
WT	Cmc1A/Cmc1D	~950	1000
STY6 (*coa6*Δ *cmc1*Δ)	Cmc1A/Cmc1D	~2000	2272
	Coa6A/Coa6D	~1800	1800
WT	Cmc3A/Cmc3D	~950	960
STY7 (*coa6*Δ *cmc3*Δ)	Cmc3A/Cmc3D	~2000	2091
	Coa6A/Coa6D	~1800	1800
WT	Cmc4A/Cmc4D	~800	800
STY8 (*coa6*Δ *cmc4*Δ)	Cmc4A/Cmc4D	~2000	2158
	Coa6A/Coa6D	~1800	1800
WT	Sco1A/Sco1D	~1450	1542
STY9 (*coa6*Δ *sco1*Δ)	Sco1A/Sco1D	~2000	2105
	Coa6A/Coa6D	~1800	1800
WT	Sco2A/Sco2D	~1550	1661
STY10 (*coa6*Δ *sco2*Δ)	Sco2A/Sco2D	~2100	2238
	Coa6A/Coa6D	~1800	1800
WT	Pic2A/Pic2D	~1100	1185
STY11 (*coa6*Δ *pic2*Δ)	Pic2A/Pic2D	~1900	1866
	Coa6A/Coa6D	~1800	1800

High-throughput phenotypic analysis of yeast strains

WT and selected mutant strains were precultured in 2 ml of YPD media in snap cap tubes for 16 to 20 hours at 30°C and 250 RPM. Cell number of overnight precultured yeast strains were counted by hemocytometer and were serially diluted at 10^4, 10^3, 10^2, and 10^1 cells per 1.5 µl in 1.7 mL eppendorf tubes. 200 µl of each diluted yeast strain was transferred into the corresponding well of a 96 deep-well plate (E&K Scientific EK-36261). The remaining seventy-two wells received 180 µl of autoclaved water, and a multichannel pipette (Eppendorf 3122000043) was used to make 1:10 serial dilutions. The 96 pin deep-well replicator (V&P Scientific 407AM) was cleaned prior to stamping with cleaning solution (V&P Scientific 110), distilled water, and ethanol, followed by flaming. Nunc OmniTray rectangular solid media plates (Thermo Scientific 242811) were obtained. A library copier (V&P Scientific 381A) and as a colony copier (V&P Scientific 380) were used to ensure even replicator insertion into the 96 deep well plate and application to the media, respectively. Following application of yeast to media, the plates were incubated at 30°C or 37°C for three to five days.

CHAPTER III

RESULTS

Coa6 is required for respiration in yeast *Saccharomyces cerevisiae*

Because of the ease of performing biochemical and functional genomic experiments, we utilized *S. cerevisiae* as a model system to uncover the role of Coa6 in mitochondrial energy metabolism. Yeast with deletion in MRC genes are viable because in the presence of glucose yeast preferentially generate cellular energy through fermentation, bypassing the need for a functional MRC. This property of yeast makes it an attractive model system to use when studying MRC biogenesis. A defect in the MRC can be revealed when yeast are forced to generate cellular energy using the mitochondria by growing them in the presence of a non-fermentable carbon source, such as glycerol or ethanol. We began our experiments by extensively characterizing the growth of *coa6Δ* yeast cells in different carbon sources and at varying temperatures. Yeast prefer to grow at 30°C, so growing the yeast at a higher temperature, such as 37°C, can add stress that may expose a phenotype too subtle to observe at 30°C. The growth of *coa6Δ* cells in liquid glucose-containing fermentable medium (YPD), as measured by spectrophotometry, is comparable to wildtype (WT) up to the early stationary phase, approximately twelve hours (Fig. 3A). At this point, the yeast have metabolized all available glucose into ethanol via fermentation pathways, and continued growth can only be achieved by shifting energy metabolism to process ethanol using the MRC. The *coa6Δ* cells have reduced growth in the stationary phase in YPD media compared to WT, indicating their inability to make this metabolic shift due to a defect in mitochondrial energy metabolism (Fig. 3A). Furthermore, in liquid glycerol/ethanol-containing,

non-fermentable medium (YPGE), *coa6Δ* demonstrates impaired growth and an extended lag phase compared to WT, indicating that the yeast possess a defective MRC (Fig. 3B). As expected, the growth of *coa6Δ* in solid YPD medium was comparable to WT, but the growth in solid YPGE was reduced, with the effect being more severe at 37°C (Fig. 3C). The growth defect of *coa6Δ* cells in non-fermentable media suggested respiratory deficiency. To directly assess respiration, we measured oxygen consumption in WT and *coa6Δ* cells and observed a statistically significant 50% decrease in the oxygen consumption rate (OCR) of *coa6Δ* cells compared with WT cells (Fig. 3D).

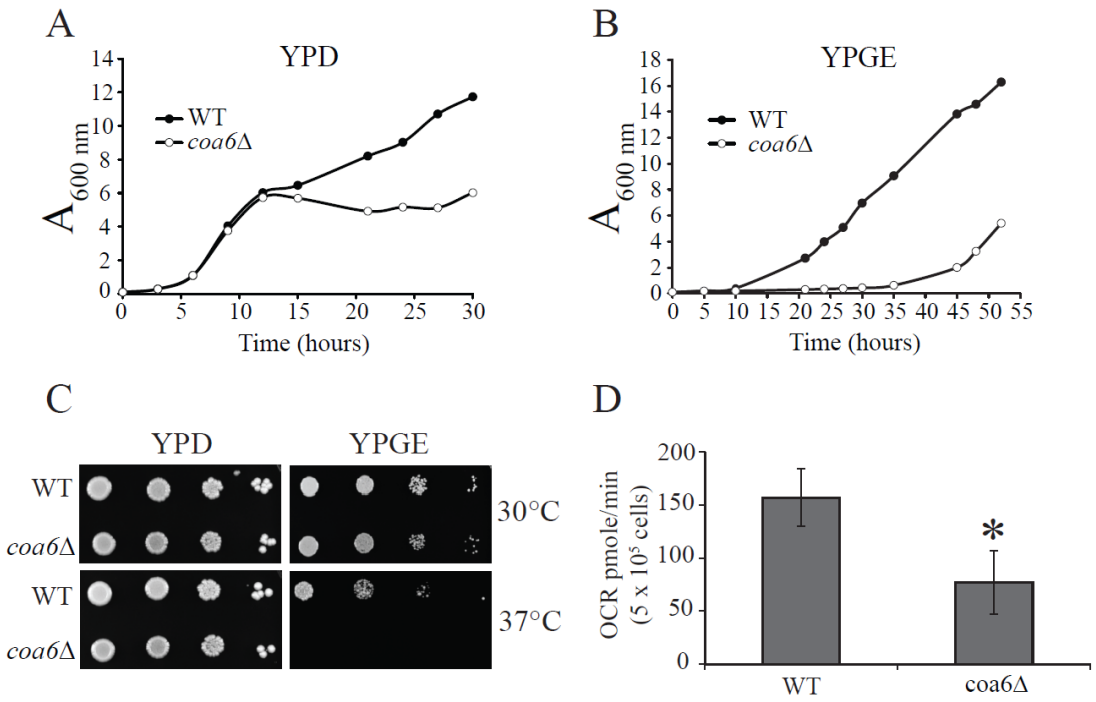

Figure 3. Yeast *coa6Δ* cells exhibit reduced respiration. (A) WT and *coa6Δ* cells were precultured in YPD and inoculated in fresh YPD liquid media at 30°C with a starting A_{600} of 0.1. Absorbance was measured at the indicated times at 600 nm. Data are representative of at least three independent measurements. (B) WT and *coa6Δ* cells were precultured in YPD and inoculated in fresh YPGE liquid media at 30°C with a starting A_{600} of 0.1. Absorbance was measured at the indicated times at 600 nm. Data are representative of at least three independent measurements. (C) Serial dilutions of WT and *coa6Δ* cells were spotted on YPD and YPGE plates at 30°C and 37°C. Pictures were taken after 2–5 days of spotting. Data are representative of three independent experiments. (D) WT and *coa6Δ* cells were grown overnight in YPD at 30°C. After 18 h of growth, cells were harvested, washed, counted and resuspended in ethanol-containing respiratory medium. Basal oxygen consumption rate (OCR) was measured on half a million cells using an extracellular flux analyzer. Error bars represent mean + SD (n = 10); ∗ denotes statistically significant differences, $P < 0.001$, *t-test*.

Coa6 is required for MRC complex IV assembly

In order to unravel the biochemical basis of the reduced respiration of *coa6Δ* cells, we performed a Western blot analysis of MRC proteins from WT and *coa6Δ* cells under denaturing conditions (SDS-PAGE). We observed a specific reduction in MRC Complex IV, also known as Cytochrome *c* Oxidase (CcO), by probing for CcO subunits Cox2 and Cox3 (Fig. 4). There was no alteration in the subunits of any other MRC complexes. Taken together, these results demonstrate that Coa6 is required for CcO assembly.

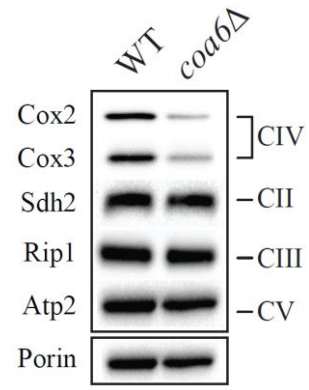

Figure 4. Yeast *coa6Δ* cells exhibit diminished CcO assembly. Mitochondria were isolated from WT and *coa6Δ* cells grown to early stationary phase in YPD medium. Mitochondrial protein was extracted and analyzed by SDS-PAGE/Western blot. Subunit-specific antibodies were used to detect MRC complexes II–V. Porin was used as loading control.

Coa6 contains an evolutionarily conserved Cx_9C-$Cx_{10}C$ motif

Having implicated Coa6 in the biological process of CcO biogenesis, we sought to further characterize Coa6 and determine its molecular function. For this, we analyzed the amino acid sequence alignment of Coa6 across five different model systems: yeast (*Saccharomyces*

cerevisiae), fly (*Drosophila melanogaster*), fish (*Danio rerio*), rat (*Rattus norvegicus*), and humans (*Homo sapiens*). Our analysis showed that Coa6 contains a non-canonical conserved Cx_9C-$Cx_{10}C$ motif (Fig. 5). The importance of this motif was underscored not only due to its evolutionary conservation, but also due to the fact that the mutations in the mitochondrial disease patient were identified in this motif (7) (Fig. 5). This evolutionarily conserved Cx_9C-$Cx_{10}C$ motif is highly similar to the twin Cx_9C motif found in a group of mitochondrial proteins which, like Coa6, are known to localize to the mitochondrial intermembrane space (IMS) (10), and have been studied for their role in MRC biogenesis, specifically through the delivery of copper (Cu) ions to CcO (9,11).

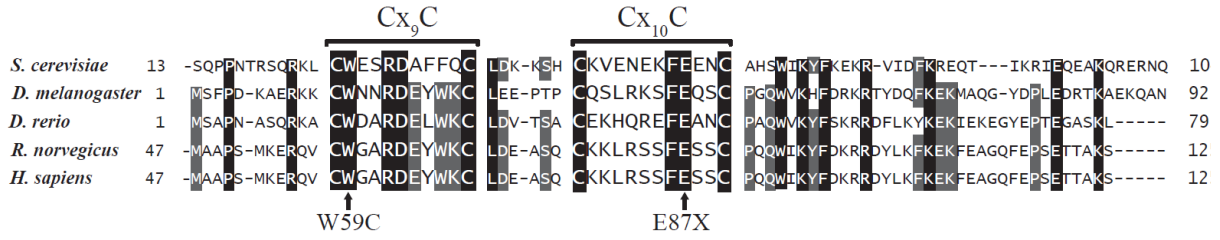

Figure 5. COA6 contains an evolutionarily conserved Cx_9C-$Cx_{10}C$ motif. Sequence alignment of the conserved region of the human COA6 protein with its orthologs in yeast (*Saccharomyces cerevisiae*), fly (*Drosophila melanogaster*), fish (*Danio rerio*), and rat (*Rattus norvegicus*). The sequence alignment was performed using ClustalW. Horizontal lines above Cx_9C and $Cx_{10}C$ residues show the conserved motif. Arrows indicate amino acid residues (tryptophan 59 and glutamic acid 87) that were mutated in the mitochondrial disease patient (7).

Exogenous copper supplementation rescues the respiratory growth defect of *coa6Δ* cells

The identification of a conserved, non-canonical Cx_9C-$Cx_{10}C$ motif in Coa6 suggested that it acts similarly to the previously identified Cx_9C proteins and plays a role in the delivery of Cu to CcO. The deletion of Cox17, a well characterized twin Cx_9C protein and a known Cu metallochaperone, results in decreased CcO levels and a loss of respiratory growth in yeast (12).

However, growth in these cells can be restored by the addition of exogenous copper salts (12). We asked whether exogenous Cu supplementation could rescue the growth defect of *coa6Δ* cells. Remarkably, Cu supplementation completely restored respiratory growth in *coa6Δ* cells in both solid and liquid media (Fig. 6A & B). Notably, the rescue was specific to Cu, as supplementation with the other bivalent metals, including cobalt, magnesium, and zinc, failed to rescue the respiratory growth defect (Fig. 6A & B). The depletion of Cu in synthetic media with an extracellular copper-specific chelator, bathocuproinedisulfonic acid, completely inhibited the growth of *coa6Δ* cells on non-fermentable medium, even at 30°C (Fig. 6C). These results implicate Coa6 in mitochondrial Cu metabolism and transport to CcO.

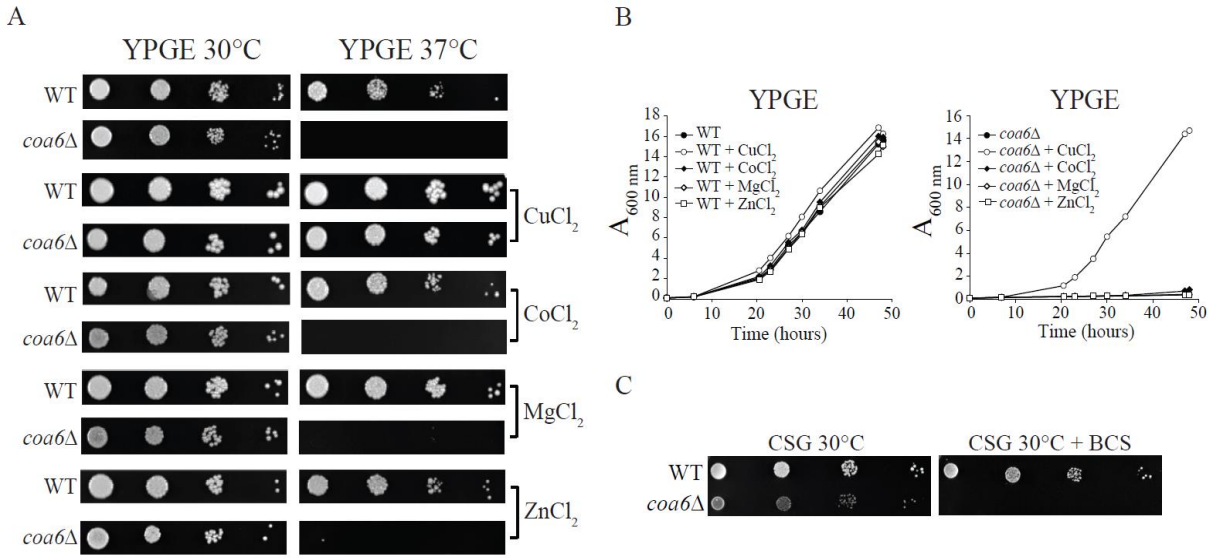

Figure 6. Cu supplementation rescues the respiratory growth defect of *coa6Δ*. (A) Serially diluted WT and *coa6Δ* cells were spotted on YPGE plates in the presence and absence of 5 µM Cu, Co, Mg and Zn bivalent salts at 30°C and 37°C and allowed to grow for 4 –5 days before imaging. (B) Growth of WT and *coa6Δ* cells in YPGE liquid media in the presence of 5 µM Cu, Co, Mg and Zn bivalent salts at 30°C. (C) Serial dilutions of WT and *coa6Δ* strains grown in synthetic medium with a non-fermentable carbon source (2% glycerol; CSG) with or without 20 µM bathocuproinedisulfonic acid (BCS). The pictures were taken 5 days after seeding.

Point mutations in the conserved Cx_9C-$Cx_{10}C$ motif disrupt Coa6 function

Following the discovery that Cu supplementation restores the growth of *coa6Δ* cells, we sought to interrogate the importance of the Cx_9C-$Cx_{10}C$ for the function of Coa6. The mutations in the mitochondrial disease patient presented in the Cx_9C-$Cx_{10}C$ motif as a missense mutation in the conserved tryptophan residue (p.W59C) and a nonsense mutation in the conserved glutamic acid residue (p.E87X) (7) (Fig. 7A). In order to test the requirement of the conserved cysteines and the effect of the patient mutations on Coa6 function, we cloned yeast COA6 into the Gateway expression vector pAG423GPD-ccdB-HA and performed site-directed mutagenesis to replace each of the four cysteines of the Cx_9C-$Cx_{10}C$ motif with alanines. Cysteines contain a thiol functional group, which are known to coordinate Cu ions. Replacing the cysteines with alanines, which do not contain thiols, represent a sufficient alteration in the function of the amino acid to assess the requirement of the cysteines for protein function. We also replaced the conserved tryptophan with a cysteine (p.W26C) to mimic the first patient mutation (p.W59C). The second patient mutation (p.E87X) is a nonsense mutation that results in a truncated protein devoid of the fourth conserved cysteine, which is mimicked by the construct with a Coa6 (p.C68A) mutation. While WT COA6 rescued the respiratory growth defect of *coa6Δ* cells, none of the point mutations in conserved residues, including the patient mutation, could rescue the respiratory growth phenotype, suggesting their critical requirement for Coa6 function (Fig. 7B). Notably, growth was most deficient in the yeast strain whose constructs corresponded to the nonsense patient mutation. These results confirm the importance of the Cx_9C-$Cx_{10}C$ motif for protein function, and suggest that the mutations reported in the described mitochondrial disease patient likely played a causal role in the disease pathogenesis.

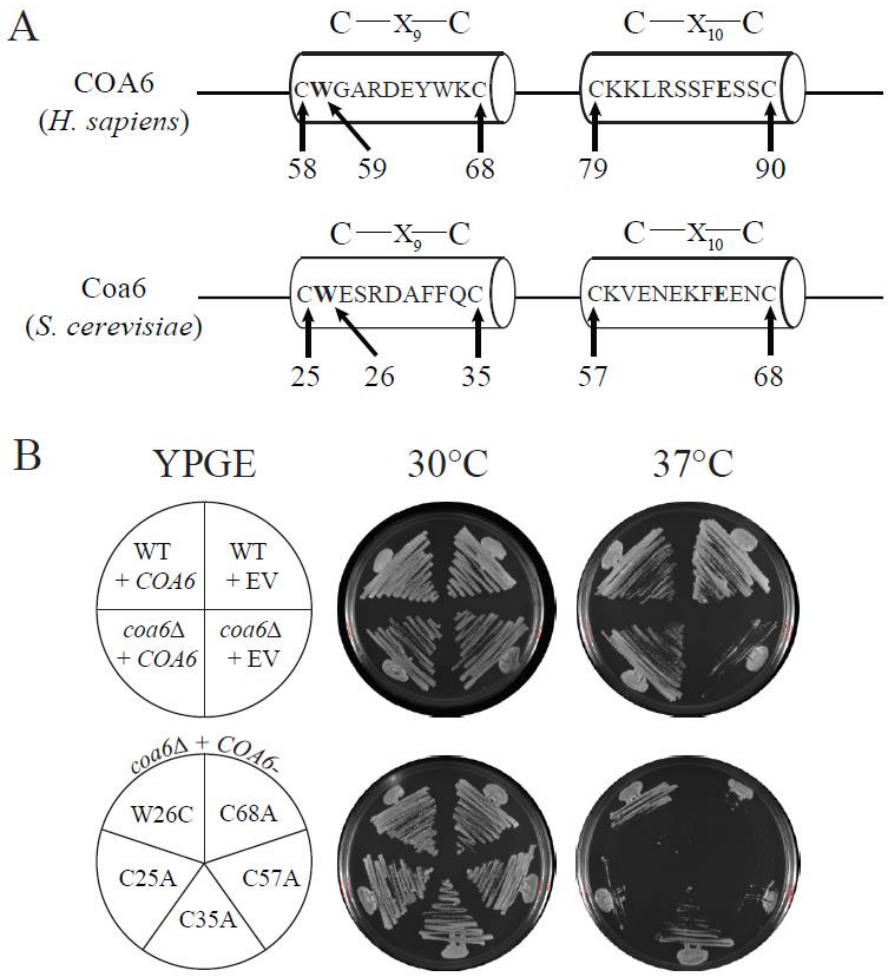

Figure 7. Conserved residues in the Cx_9C-$Cx_{10}C$ motif are essential for protein function. (A) Schematic representation of the Cx_9C-$Cx_{10}C$ motif of human COA6 and yeast Coa6 proteins showing the location of cysteine and tryptophan residues (arrows) targeted for site-directed mutagenesis. (B) WT and *coa6Δ* cells transformed with empty vector (EV), *COA6*, or one of its mutant forms were streaked onto YPGE plates and incubated at 30°C or 37°C for 5 days before imaging.

COA6* is synthetic sick with *SCO2* and *COX12

After demonstrating the necessity of the Cx_9C-$Cx_{10}C$ motif for the function of Coa6 and implicating the protein in the delivery of Cu to CcO, we sought to further analyze the genetic interaction between Coa6 and assembly factors also hypothesized to play a role in the delivery of Cu to CcO. We constructed a *coa6Δ*::clonNAT strain in MATα background and mated it with

MATa KANMX4 knockout strains for Cox11, Cox12, Cox19, Cox23, Cmc1, Cmc3, Cmc4, Sco1, Sco2, and Pic2, as well as a MATa hygro knockout strain for Cox17. The genotypes were confirmed by replica plating (Table 1), and successful chromosomal gene deletions were confirmed by PCR (Table 3). Each of these proteins either contains a twin Cx_9C motif (9), a Cx_9C-$Cx_{10}C$ motif (13), or has been implicated in mitochondrial Cu metabolism (9,14). The resulting heterozygous diploids were sporulated, and meiotic tetrad analysis was carried out. Three independent tetrad counts were performed for each double knockout construct, and the relative frequency of tetrad formation indicated the genetic viability of the double knockouts (Fig. 8). Notably, *cox12Δcoa6Δ*, *cox17Δcoa6Δ, sco1Δcoa6Δ, sco2Δcoa6Δ,* and *pic2Δcoa6Δ* showed a significant decrease in tetrad formation, indicating that these double knockouts possessed a much lower fitness than other double knockouts or WT (Fig. 8).

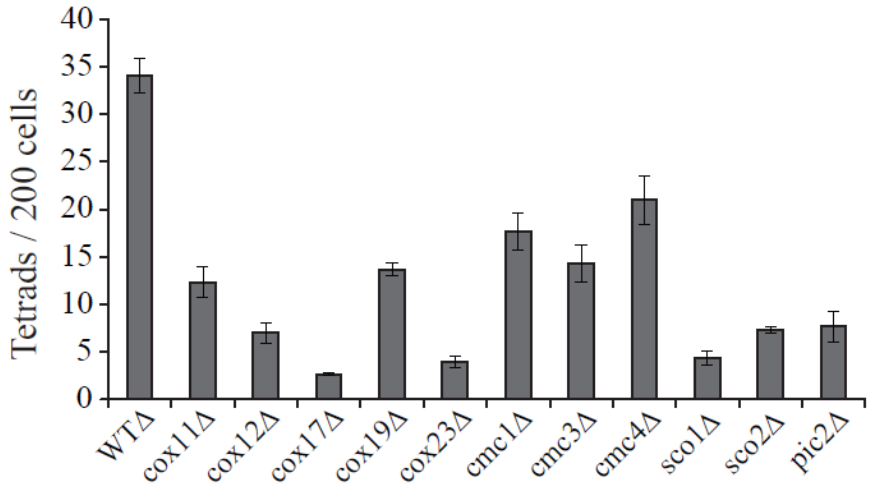

Figure 8. The fitness of the double knockouts demonstrates genetic interaction between *COA6* and CcO assembly factors. Haploid single knockouts of opposite mating types were mated, precultured overnight in YPD, and sporulated. The number of tetrads per 200 cells on day 5 was quantified by hemocytometer. Data reflects three independent trials.

A high-throughput growth experiment was designed in which four serial dilutions of WT, *coa6Δ, cox11Δ, cox12Δ, cox17Δ, cox19Δ, cox23Δ, cmc1Δ, cmc3Δ, cmc4Δ, sco1Δ, sco2Δ,* and *pic2Δ*

strains, as well as the eleven double knockout strains (Table 1), were made in a 96 deep well plate. The yeast were stamped onto synthetic media containing glucose, galactose, or glycerol, and grown at 30°C or 37°C for three to five days. Galactose was chosen as a respiro-fermentative media since galactose does not activate the carbon catabolite repression pathways that prevent mitochondrial biogenesis when yeast are grown in the presence of glucose (15). The layout of the stamping plate and an example of a synthetic glucose stamping experiment are displayed (Fig 9A). In order to identify genetic interactions between *COA6* and other CcO assembly factors implicated in mitochondrial Cu metabolism, we performed the high-throughput phenotypic analysis by searching for double knockouts whose growth defect was more severe than the growth defect of the least proliferating parent strain. Growth was measured by counting the number of serial dilutions which had grown on the solid media plate. All strains grew well in glucose containing media at 30°C, indicating that the deletion of *COA6* in addition to genes for other CcO assembly factors was not lethal in fermentable conditions (Fig. 9B). In galactose containing synthetic media, *COA6* demonstrated synthetic sick interaction with both *COX12* and *COX23*, and in glycerol containing synthetic media, *COA6* demonstrated synthetic sick interaction with *SCO2*, *CMC1*, and *CMC3* (Fig. 9B). An additional phenotypic analysis was carried out to score the growth of the double knockouts of *COA6* with *COX12* and *SCO2*. A spotting analysis on synthetic galactose and glycerol media with and without Cu supplementation showed that *cox12Δcoa6Δ* and *sco2Δcoa6Δ* have severe growth defects beyond the growth defects of *coa6Δ, sco2Δ,* or *cox12Δ* (Fig. 9C & D). Additionally, neither double knockout's growth was rescued by Cu supplementation (Fig. 9C & D), suggesting that Sco2 and Cox12 act downstream of or parallel to Coa6 in the Cu delivery pathway to CcO.

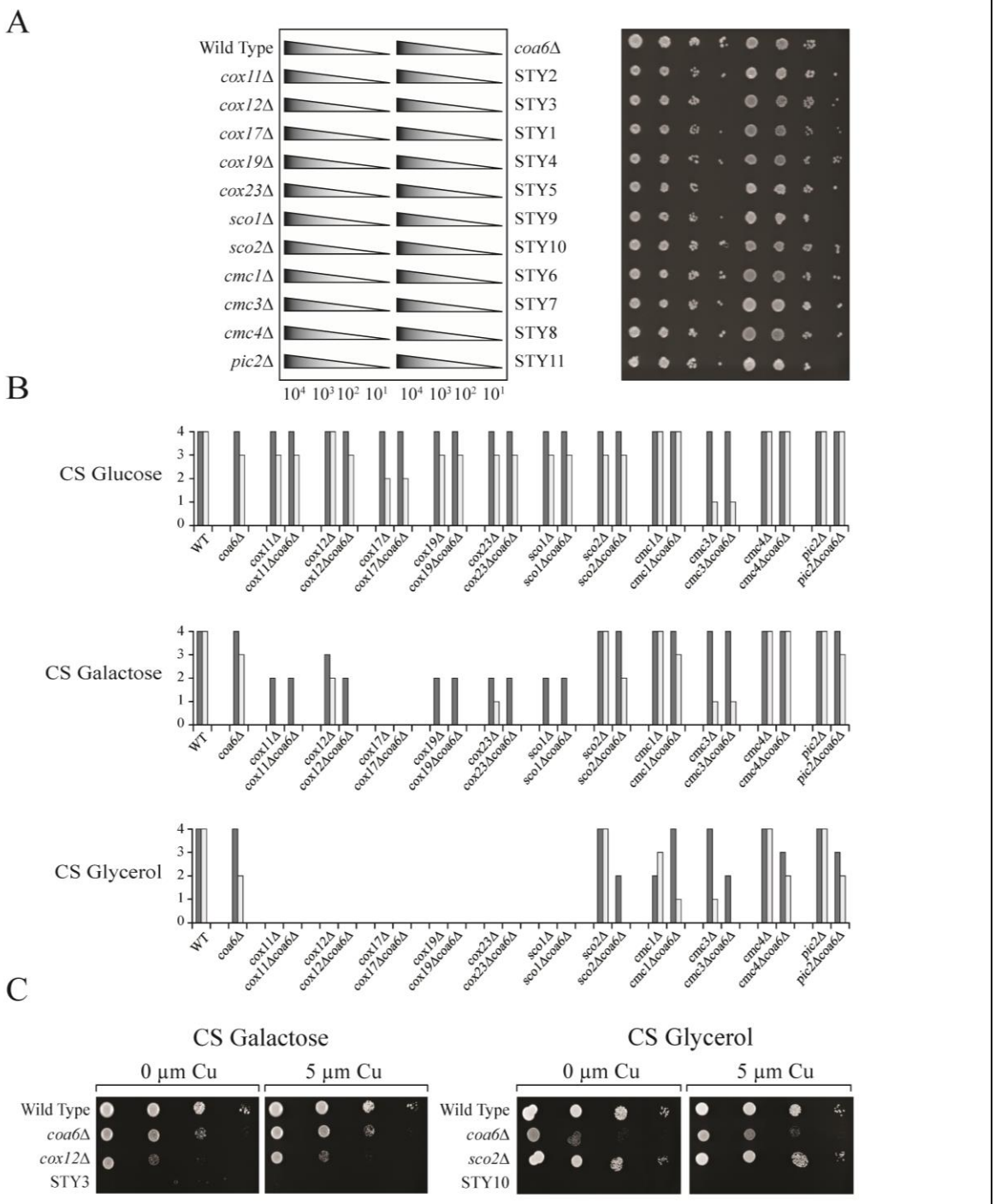

Figure 9. High-throughput phenotypic analysis of double knockouts reveals synthetic sick phenotypes. (A) Schematic indicating the position and concentration of yeast strain dilutions on rectangular media next to a synthetic glucose example. (B) Growth analysis of double knockouts relative to WT and parent strains on glucose, galactose, and glycerol containing synthetic media at 30°C or 37°C after three to five days. (C) Spotting analysis demonstrates *cox12Δcoa6Δ* and *sco2Δcoa6Δ* possess a respiratory growth defect on galactose and glycerol media, respectively, and are not rescued by exogenous Cu supplementation.

CHAPTER IV

DISCUSSION

Despite the fundamental importance of the MRC in cellular energy production and human health, many of the factors required for its biogenesis are still unknown. To address this gap in our knowledge of mitochondrial biogenesis, we used an integrative approach based on clues from evolutionary history, protein localization studies, and human genetics to identify novel putative MRC biogenesis factors. Mutations in one of our prioritized candidates, *C1orf31*/*COA6*, were identified in a mitochondrial disease patient (7), suggesting its critical importance for MRC function and/or formation. Detailed experimental analysis using a yeast knockout model of COA6 deficiency showed its critical requirement for mitochondrial respiration and CcO biogenesis. The specific requirement of Coa6 for CcO biogenesis, its intramitochondrial localization (10), and the presence of an evolutionarily conserved Cx_9C-$Cx_{10}C$ motif suggested a role in mitochondrial Cu metabolism (9,11). In support of this, we show that exogenous Cu supplementation completely rescues the respiratory defect in yeast *coa6Δ* cells (Fig. 6), and the conserved residues within the putative, non-canonical Cu binding Cx_9C-$Cx_{10}C$ motif are essential for protein function (Fig. 7). Furthermore, we identified synthetic sick interaction of *COA6* with known Cu metallochaperones (Fig. 9). Taken together, our study shows that Coa6 is an evolutionarily conserved MRC biogenesis factor that facilitates CcO assembly by regulating mitochondrial Cu metabolism.

In our search for novel MRC biogenesis factors, we chose to focus on *COA6* because three independent lines of evidence linked it to MRC function. First, it is an evolutionarily conserved

protein that localizes to yeast and mammalian mitochondria (10,6). Second, previous genomic and proteomic studies in yeast have shown that Coa6 plays a role in CcO assembly and interacts with known MRC components (16,10). Third, potential pathogenic mutations were reported in the conserved residues of *COA6* in a mitochondrial disease patient (7). Utilizing a knockout model in the yeast *S. cerevisiae*, we showed that Coa6 is essential for the maintenance of steady-state levels of CcO (Fig. 4) and its deficiency results in reduced respiration (Fig. 3D). The patient mutations were present within conserved residues of the evolutionarily conserved Cx_9C-$Cx_{10}C$ motif, suggesting their essential function (7) (Fig. 5). We generated point mutations in the yeast Coa6 protein that were synonymous to compound heterozygous mutations reported in the human patient, and showed that mutant proteins failed to rescue the respiratory deficient growth of *coa6Δ* cells (Fig. 6B), thus establishing the pathogenicity of the patient mutations, as well as confirming the functional requirement of the Cx_9C-$Cx_{10}C$ motif.

The evolutionarily conserved, non-canonical Cx_9C-$Cx_{10}C$ motif of Coa6 is similar to the twin Cx_9C motif found in a subset of mitochondrial IMS involved in Cu delivery to CcO (9). The rescue of respiratory growth defect of yeast *coa6Δ* cells with exogenous Cu supplementation suggests a role for Coa6 in the Cu-delivery pathway to CcO. Notably, genetic mutations in three IMS proteins, the mitochondrial Cu metallochaperones, Sco1 and Sco2, and a twin Cx_9C protein C2orf64/COA5, have been previously reported in mitochondrial disease patients with pronounced CcO deficiency and distinct, early-onset fatal clinical phenotypes (17-19). Patients with *SCO1* mutations suffer from neonatal hepatic failure and ketoacidotic coma, whereas *SCO2* and *COA5* mutations are associated with fatal neonatal cardiomyopathy. The clinical symptoms of the *COA6* mutations are thus similar to *SCO2* and *COA5* patient mutations, suggesting that

these proteins partake in a common biochemical process. This idea is further strengthened by the respiratory genetic synthetic sick interaction of *COA6* and *SCO2* (Fig. 9B & C). Interestingly, Cu supplementation has been shown to rescue CcO activity in patient-derived *SCO2* mutant cells, as well as improve the clinical symptoms of patients suffering from aberrant mitochondrial Cu metabolism (20). Our demonstration of Cu rescue of *coa6Δ* yeast cells motivates further investigation of Cu-mediated rescue of COA6 deficiency in mammalian cells.

Although Cu supplementation offers an exciting therapeutic avenue for mitochondrial patients with aberrant mitochondrial Cu metabolism, many important questions regarding the mechanism of Cu-mediated rescue and the Cu-delivery pathway remain unanswered. For example, why and how is Cu supplementation able to bypass the complete absence of a Cu metallochaperone? Why are there so many IMS proteins in the Cu delivery pathway? Despite the discovery of several IMS Cu-binding proteins over the last decade and a half, our understanding of the mitochondrial Cu delivery pathway to CcO subunits remains incomplete. In *S. cerevisiae*, up to ten proteins (Cox11, Sco1, Sco2, Cox17, Cox19, Cox23, Cmc1, Cmc2, Pet191, and Pic2) have been implicated so far in the Cu delivery pathway to CcO (11,14). It has been suggested that in a daisy chain transfer mechanism, Cu is successively transferred from its non-protein ligand in the mitochondrial matrix to the IMS proteins for final delivery to Cox1 and Cox2 (11) (Fig. 10A). However, only the last few steps that involve successive transfer of Cu from Cox17 to Cox1 and Cox2 via Cox11 and Sco1, respectively, are well characterized (21,22).

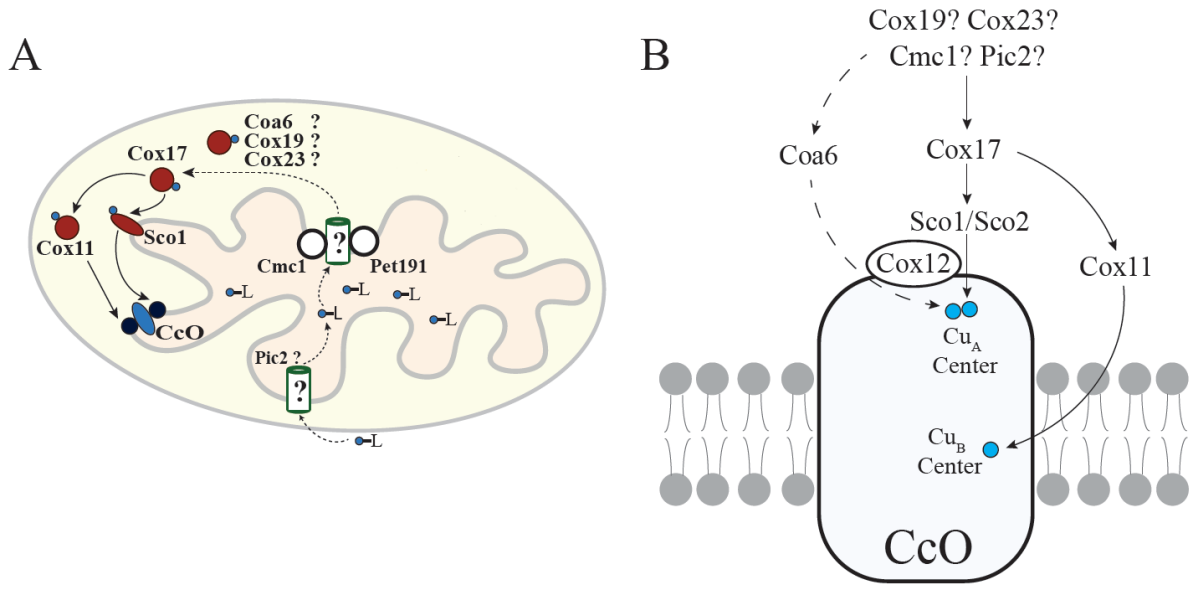

Figure 10. Mitochondrial Cu metabolism. (A) Schematic of the proposed mitochondrial Cu transport pathways to CcO subunits. Cu (blue circles) enters the mitochondrial matrix bound to an unidentified ligand (-L) partially through the recently identified Pic2 protein. Cu is stored in the matrix and exported to the intermembrane space to be delivered to CcO through a series of metallochaperones depicted in red. Only the final steps of Cu delivery mediated by Cox17, Cox11 and Sco1 are experimentally demonstrated. Dashed arrows indicate the hypothetical role of the several Cx_9C containing proteins, including Coa6, in Cu transfer from a matrix Cu pool, across the inner mitochondrial membrane, to CcO. (B) Proposed parallel pathway of Coa6-mediated Cu delivery to the Cu_A site of CcO.

The current hypothesis in the field of mitochondrial Cu trafficking is that the proteins which participate in Cu delivery to CcO transfer Cu ions in a linear pathway, eventually reaching Cox17 (9). Cox17 then donates Cu to Cox11 and Sco1, which successively metallate Cox1 and Cox2, respectively. However, a number of observations do not support this linear model of Cu trafficking in the IMS. For example, the growth of yeast knockouts for Cox17 and Cmc1, twin Cx_9C Cu metallochaperones, can be rescued by exogenous Cu supplementation (9,23). This is unlikely in a linear pathway, and suggests the presence of parallel pathways of Cu delivery to CcO, a far more evolutionarily favorable model considering the essential role of CcO in mitochondrial energy generation. Additionally, recent *in vitro* Cu transfer experiments between purified bacterial Sco proteins and Cox2, which contains the Cu_A site in eukaryotic CcO, do not proceed to completion (24). This evidence suggests that the final steps of Cox2 metallation

require additional and as-of-yet unidentified Cu metallochaperones. We predict Coa6 to be either a regulator or a bona fide member of the Cu-delivery pathway to CcO because of the presence of the highly conserved Cx_9C-$Cx_{10}C$ motif, its localization to the IMS, and the rescue a respiratory growth defect in yeast *coa6Δ* cells by exogenous Cu supplementation. The diminished tetrad formation from sporulation of double knockouts between Coa6 and proteins known to be involved in Cu delivery to Cox2 suggest that Coa6 participates specifically in this facet of mitochondrial Cu metabolism. Most notably, however, is the finding that the double knockout between Coa6 and Sco2 cannot be rescued by exogenous Cu supplementation. This suggests that Coa6 participates in either a parallel pathway of Cu delivery to CcO, whose absence can be compensated for by the addition of exogenous Cu, or acts upstream of Sco2 (Fig. 10B).

Much remains to be determined concerning mitochondrial Cu metabolism. The full characterization of the pathway by which CcO receives its Cu cofactors is an important objective, as it will not only fundamentally enhance the field of mitochondrial biology, but may also yield information about which mitochondrial disease patients may benefit from treatment by Cu supplementation. Elucidation of the role of Coa6 in mitochondrial energy generation is the proof-of-principle of our combined computational, genetic, and biochemical strategy to identify novel MRC biogenesis factors, and will bring the field of mitochondrial medicine one step closer to understanding the full complement of genes required for building the mitochondrial energy generating machinery.

REFERENCES

1. Calvo SE, Mootha VK. The mitochondrial proteome and human disease. Annu Rev Genomics Hum Genet. 2010, 11:25-44. PMID: 20690818.
2. Ghezzi D, Zeviani M. Assembly factors of human mitochondrial respiratory chain complexes: physiology and pathophysiology. Adv Exp Med Biol. 2012, 748:65-106. PMID: 22729855.
3. DiMauro S, Schon EA. Mitochondrial respiratory-chain diseases. N Engl J Med. 2003, 348(26):2656-68. PMID: 12826641.
4. Skladal D, Halliday J, Thorburn DR. Minimum birth prevalence of mitochondrial respiratory chain disorders in children. Brain. 2003, 126(Pt 8):1905-12. PMID: 12805096.
5. Hess DC, Myers CL, Huttenhower C, Hibbs MA, Hayes AP, Paw J, Clore JJ, Mendoza RM, Luis BS, Nislow C, Giaever G, Costanzo M, Troyanskaya OG, Caudy AA. Computationally driven, quantitative experiments discover genes required for mitochondrial biogenesis. PLoS Genet. 2009, 5(3):e1000407. PMCID: PMC2648979.
6. Pagliarini DJ, Calvo SE, Chang B, Sheth SA, Vafai SB, Ong SE, Walford GA, Sugiana C, Boneh A, Chen WK, Hill DE, Vidal M, Evans JG, Thorburn DR, Carr SA, Mootha VK. A mitochondrial protein compendium elucidates complex I disease biology. Cell. 2008, 134(1):112-23. PMCID: PMC2778844.
7. Calvo SE, Compton AG, Hershman SG, Lim SC, Lieber DS, Tucker EJ, Laskowski A, Garone C, Liu S, Jaffe DB, Christodoulou J, Fletcher JM, Bruno DL, Goldblatt J, Dimauro S, Thorburn DR, Mootha VK. Molecular diagnosis of infantile mitochondrial

disease with targeted next-generation sequencing. Sci Transl Med. 2012, 4(118):118ra10. PMCID: PMC3523805.

8. Meisinger C, Pfanner N, and Truscott KN. Isolation of yeast mitochondria. Methods Mol Biol. 2006, 313: 33–39.
9. Robinson NJ and Winge DR. Copper metallochaperones. Annu Rev Biochem. 2010, 79: 537–562.
10. Vögtle FN, Burkhart JM, Rao S, Gerbeth C, Hinrichs J, Martinou JC, Chacinska A, Sickmann A, Zahedi RP, Meisinger C. Intermembrane space proteome of yeast mitochondria. Mol Cell Proteomics. 2012, 11(12):1840-52. PMCID: PMC3518125.
11. Horn D, Barrientos A. Mitochondrial copper metabolism and delivery to cytochrome c oxidase. IUBMB Life. 2008, 60(7):421-9. PMCID: PMC2864105.
12. Glerum DM, Shtanko A, and Tzagoloff A. Characterization of COX17, a yeast gene involved in copper metabolism and assembly of cytochrome oxidase. J Biol Chem. 1996, 271:14504–14509.
13. Cavallaro G. Genome-wide analysis of eukaryotic twin CX9C proteins. Mol Biosyst. 2010, 6:2459–2470.
14. Vest KE, Leary SC, Winge DR, and Cobine PA. Copper import into the mitochondrial matrix in Saccharomyces cerevisiae is mediated by Pic2, a mitochondrial carrier family protein. J Biol Chem. 2013, 288: 23884–23892.
15. Ulery TL, Jang SH, Jaehning JA. Glucose repression of yeast mitochondrial transcription: kinetics of derepression and role of nuclear genes. Mol Cell Biol. 1994, 14:1160–1170.
16. Szklarczyk R, Wanschers BF, Cuypers TD, Esseling JJ, Riemersma M, van den Brand MA, Gloerich J, Lasonder E, van den Heuvel LP, Nijtmans LG et al. Iterative orthology

prediction uncovers new mitochondrial proteins and identifies C12orf62 as the human ortholog of COX14, a protein involved in the assembly of cytochrome c oxidase. Genome Biol. 2012, 13: R12.

17. Papadopoulou LC, Sue CM, Davidson MM, Tanji K, Nishino I, Sadlock JE, Krishna S, Walker W, Selby J, Glerum DM, Coster RV, Lyon G, Scalais E, Lebel R, Kaplan P, Shanske S, De Vivo DC, Bonilla E, Hirano M, DiMauro S, Schon EA. Fatal infantile cardioencephalomyopathy with COX deficiency and mutations in SCO2, a COX assembly gene. Nat Genet. 1999, 23(3):333-7. PMID: 10545952.
18. Valnot I, Osmond S, Gigarel N, Mehaye B, Amiel J, Cormier-Daire V, Munnich A, Bonnefont JP, Rustin P, Rötig A. Mutations of the SCO1 gene in mitochondrial cytochrome c oxidase deficiency with neonatal-onset hepatic failure and encephalopathy. Am J Hum Genet. 2000, 67(5):1104-9. PMCID: PMC1288552.
19. Huigsloot M, Nijtmans LG, Szklarczyk R, Baars MJ, van den Brand MA, Hendriksfranssen MG, van den Heuvel LP, Smeitink JA, Huynen MA, and Rodenburg RJ. A mutation in C2orf64 causes impaired cytochrome c oxidase assembly and mitochondrial cardiomyopathy. Am J Hum Genet. 2011, 88: 488–493.
20. Jaksch M, Paret C, Stucka R, Horn N, Mu¨ller-Ho¨cker J, Horvath R, Trepesch N, Stecker G, Freisinger P, Thirion C et al. Cytochrome c oxidase deficiency due to mutations in SCO2, encoding a mitochondrial copper-binding protein, is rescued by copper in human myoblasts. Hum Mol Genet. 2001, 10: 3025–3035.
21. Hiser L, Di Valentin M, Hamer AG, and Hosler JP. Cox11p is required for stable formation of the Cu(B) and magnesium centers of cytochrome c oxidase. J Biol Chem. 2000, 275: 619–623.

22. Rigby K, Cobine PA, Khalimonchuk O, and Winge DR. Mapping the functional interaction of Sco1 and Cox2 in cytochrome oxidase biogenesis. J Biol Chem. 2008, 283: 15015–15022.
23. Horn D, Al-Ali H, and Barrientos A. Cmc1p is a conserved mitochondrial twin CX9C protein involved in cytochrome c oxidase biogenesis. Mol Cell Biol. 2008, 28: 4354–4364.
24. Kelly NC and Ninian JB. Stable Cu(II) and Cu(I) Mononuclear Intermediates in the Assembly of the CuA Center of Thermus thermophilus Cytochrome Oxidase. J Am Chem Soc. 2012, 134 (39): 16401-16412.